Supplementary Figure 1

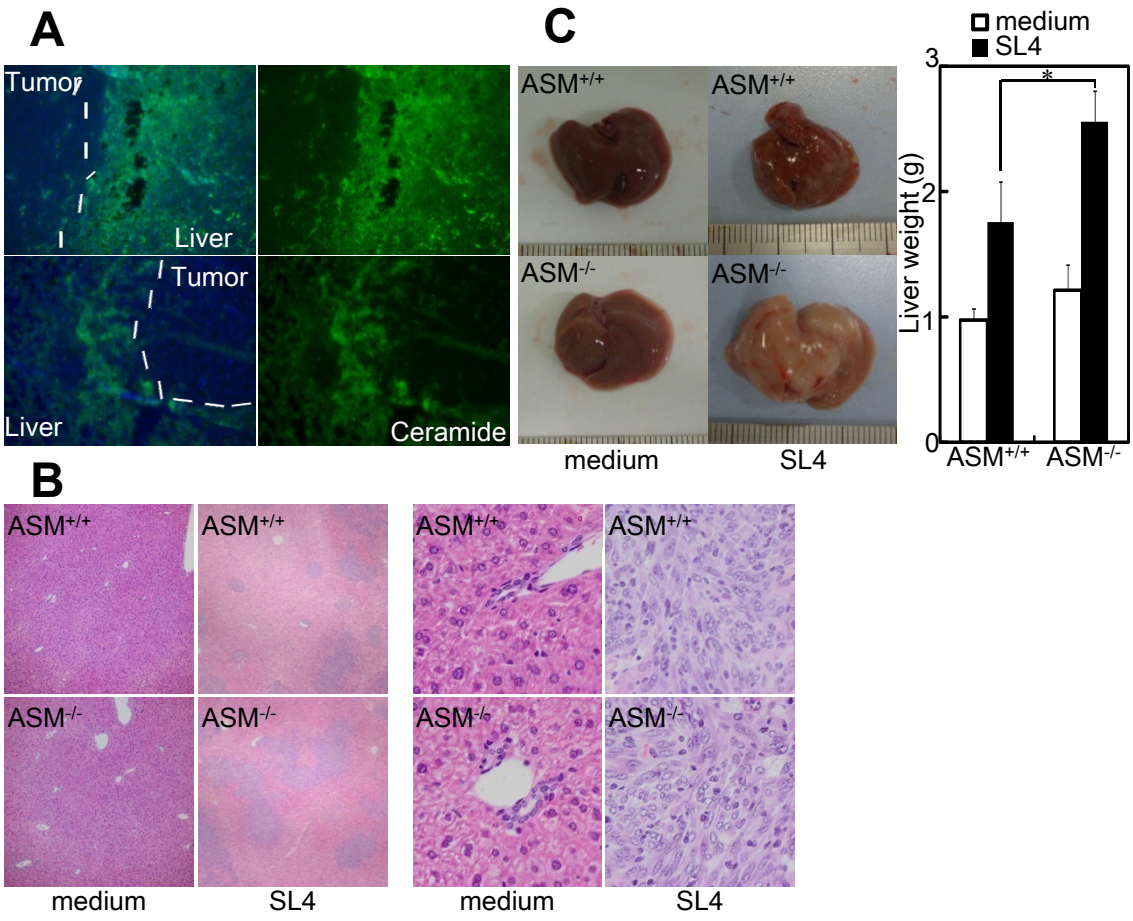

Supplementary Figure 1. ASM deficiency increased metastatic tumor growth in the liver. (A) Wild-type mice were intrasplenically injected with SL4 (2 × 10^4 cells) and sacrificed 14 d after inoculation, then the livers were excised and sections were cut on a cryostat. Expression of ASM (upper panels) and ceramide (lower panels) was examined by immunohistochemistry (right panels) with anti-ASM (Santa Cruz Biotechnology, sc-11352) and ceramide (Enzo life science, clone MID 15B4) antibodies (original magnification: 200×). Nuclei were stained with DAPI and merged with the images of cells stained with the fluorescent secondary antibodies (left panels). (B, C) *ASM*$^{+/+}$ (upper panels) and *ASM*$^{-/-}$ (lower panels) mice were intrasplenically injected with or without SL4 (5 × 10^5 cells) and sacrificed 7 d after inoculation. Liver sections were stained with H&E (B) (left panels, original magnification: 40×; right panels: 400×). Results shown are representative of 4 independent experiments. Photograph of the liver after excision and weight measurement (C). Results are presented as means ± SD of data collected from 6 independent experiments. *P < 0.05 using a 2-tailed Student's *t*-test.

Supplementary Figure 2

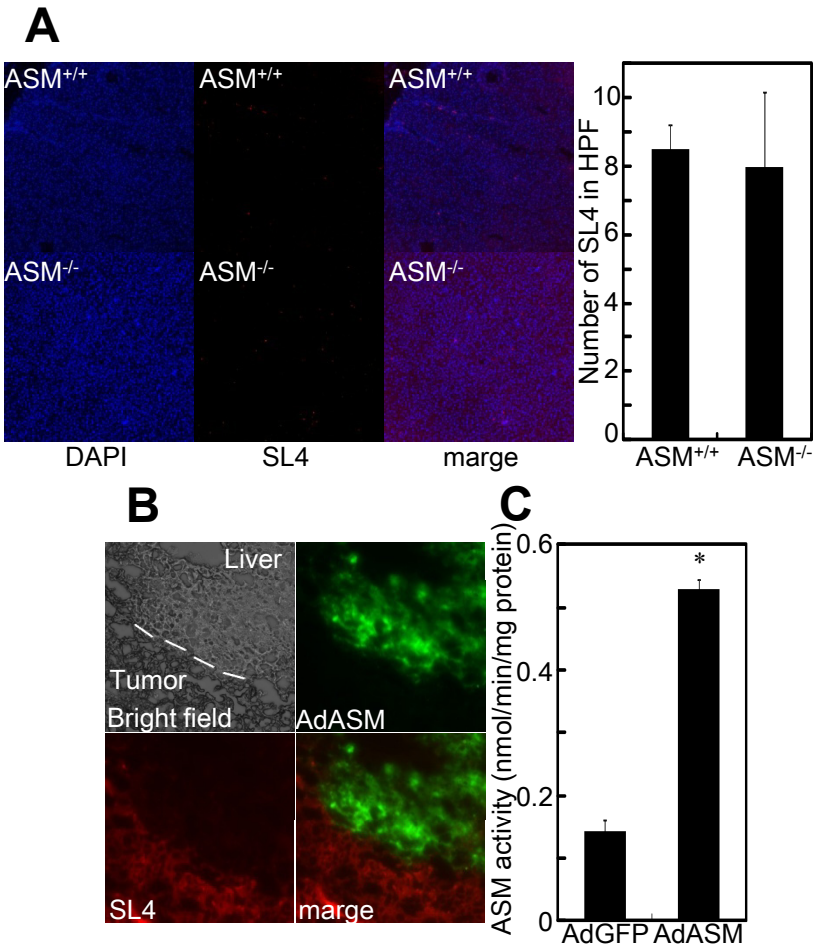

Supplementary Figure 2. AdASM infected hepatocytes and increased ASM activity. (A) *ASM*$^{+/+}$ (upper panels) and *ASM*$^{-/-}$ (lower panels) mice were intrasplenically injected with SL4 (5×10^5 cells). (B) Wild-type mice were infected with AdASM 24 h before being sacrificed 6 h (A) or 7 d (B) after SL4 inoculation. (A) For detection of RFP fluorescence, unfixed liver was embedded in OCT before frozen sections were cut on a cryostat, RFP expression of SL4 was assessed by fluorescent microscopy (original magnification: 40×), and nuclei were stained with DAPI. The number of RFP-positive cells was counted in at least 4 high-power fields (400×) on each slide and expressed as the number of cells/field. (B) AdASM-derived GFP and RFP (SL4) expression in the unfixed frozen liver was assessed by fluorescent microscopy. Each panel shows the same field of the border of the metastatic tumor and liver (original magnification: 400×). (C) After wild-type mice infected with AdGFP or AdASM had been sacrificed 3 d after infection, ASM activity in the liver was measured using [methyl-^{14}C]sphingomyelin (specific activity = 35000 dpm/assay; Amersham Pharmacia Biotech, Princeton, NJ, USA). Results shown are representative of 4 independent experiments. *$P < 0.05$ using a 2-tailed Student's *t*-test.

Supplementary Figure 3

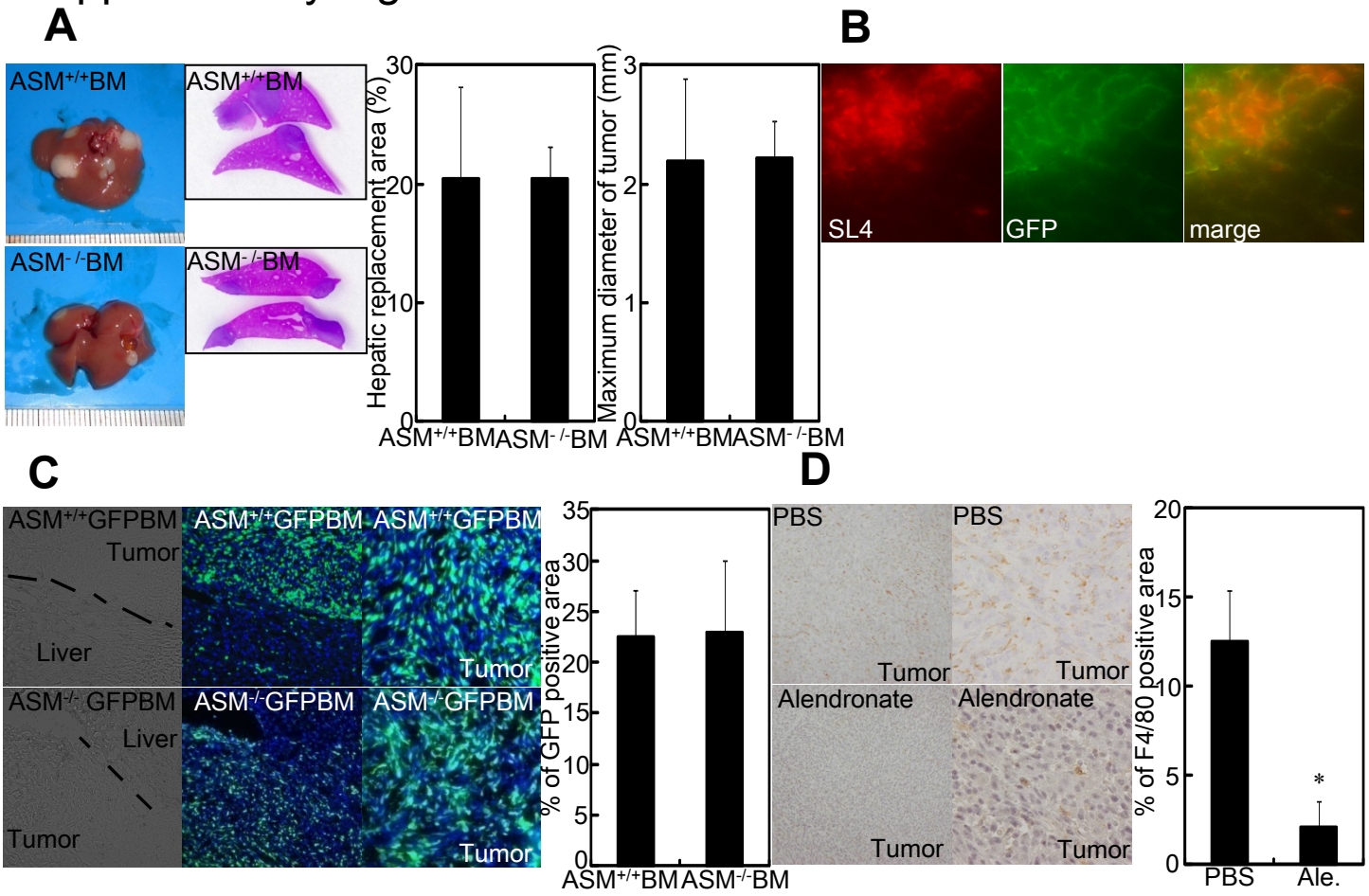

Supplementary Figure 3. ASM in bone-marrow-derived cells was not involved in increased metastatic tumor growth. All bone marrow cells from (A) *ASM*$^{+/+}$ (upper panels) and *ASM*$^{-/-}$ (lower panels) mice, (B) *GFP*$^{+}$ mice, and (C) *ASM*$^{+/+}$ *GFP*$^{+}$ (upper panels) and *ASM*$^{-/-}$ *GFP*$^{+}$ (lower panels) mice were injected into lethally irradiated wild-type recipient mice (10^7 cells). Chimeric mice were intrasplenically injected with SL4 (2×10^4 cells) 10 wk after bone marrow transplantation and sacrificed 14 d after surgery. (A) Photograph of the liver after excision. Intrahepatic tumor load was presented as hepatic replacement area and maximum diameter based on the measurements of 3 non-sequential H&E sections. (B) GFP (bone-marrow-derived cells) and RFP (SL4) expression in unfixed liver was assessed by fluorescent microscopy. (C) GFP expression in the liver was assessed by fluorescent microscopy; nuclei were stained with DAPI. Left to right: bright field at the border of the metastatic tumor and liver (original magnification: 200×), GFP/DAPI merge in the bright field (original magnification: 400×). The GFP-positive area was measured. (D) Wild-type mice were injected with SL4 cells and treated with PBS (upper panels) or alendronate (lower panels) before being sacrificed 14 d after inoculation. Expression of F4/80 in the metastatic tumor (left panels, original magnification: 100×: right panels, original magnification: 400×) was immunohistochemically examined with an anti-F4/80 antibody (graph on right panel) to assess the number of macrophages. Results are presented as means ± SD of data collected from at least 5 independent experiments. *P < 0.05 using a 2-tailed Student's *t*-test.

Supplementary Figure 4

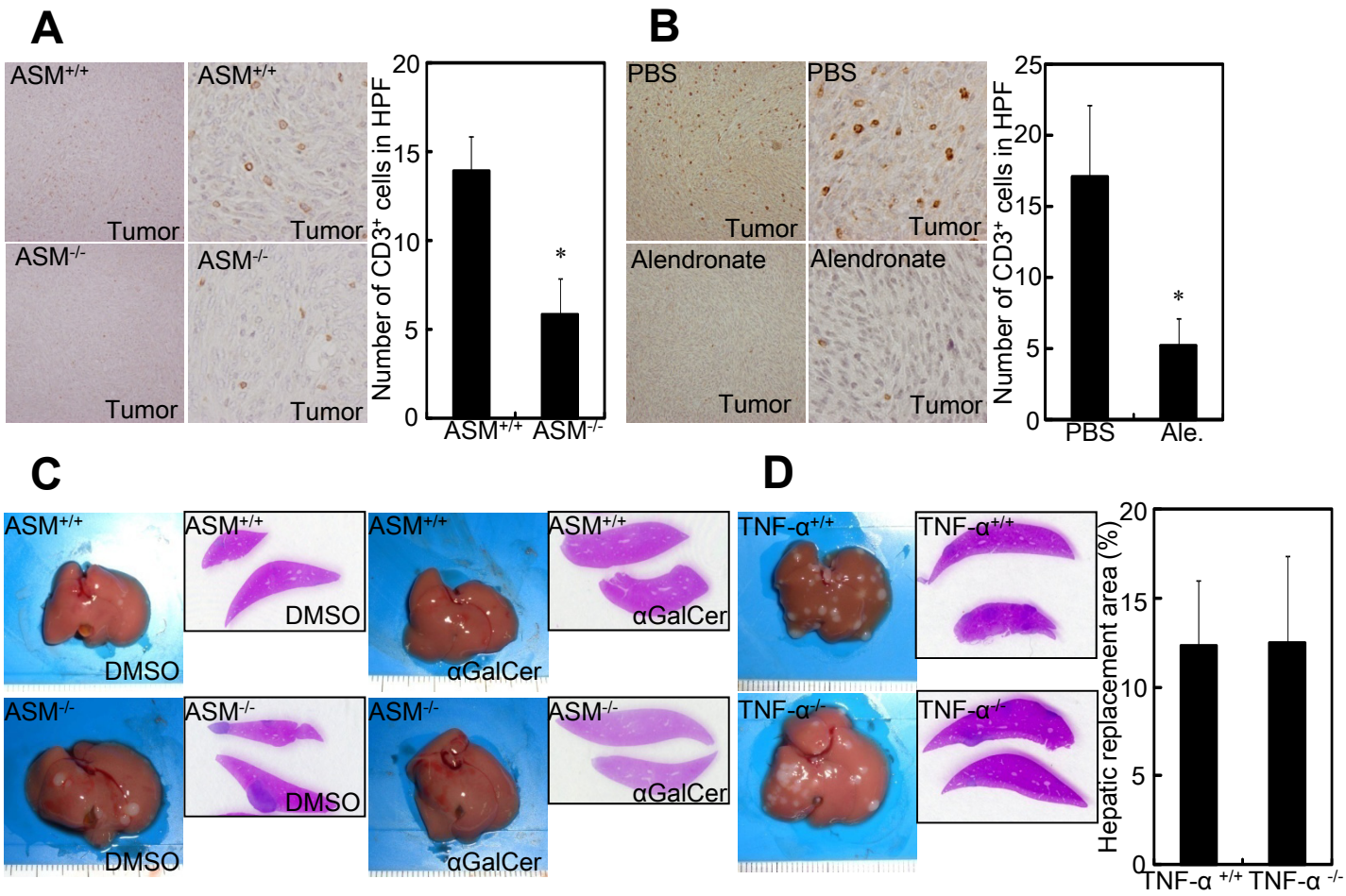

Supplementary Figure 4. TNF-α was not involved in tumor immunity. (A, C) *ASM*$^{+/+}$ (upper panels) and *ASM*$^{-/-}$ (lower panels) mice, (B) wild-type mice treated with PBS (upper panels) or alendronate (lower panels), and (D) *TNF-α*$^{+/+}$ (upper panels) and *TNF-α*$^{-/-}$ (lower panels) mice were intrasplenically injected with SL4 (2×10^4) before being sacrificed 14 d (A, B, D) after inoculation. (A, B) Expression of CD3 (original magnification, left panels: 100×; right panels: 400×) was examined by immunohistochemistry. The number of CD3 positive cells was counted in at least 4 high-power fields (400×) on each slide and was expressed as cells/field. (C) Following intraperitoneal administration of α-galactosylceramide (αGalCer, 1 μg/mouse) 24 h after inoculation, animals were sacrificed 7 d after inoculation. Photograph of the liver after excision. Liver sections were stained with H&E (loupe magnification). (D) Photograph of the liver after excision. Liver sections were stained with H&E (loupe magnification) and intrahepatic tumor load was presented as hepatic replacement area based on the measurement of 3 non-sequential sections. Results are presented as means ± SD of data collected from at least 5 independent experiments. *$P < 0.05$ using a 2-tailed Student's *t*-test.

Supplementary Figure 5

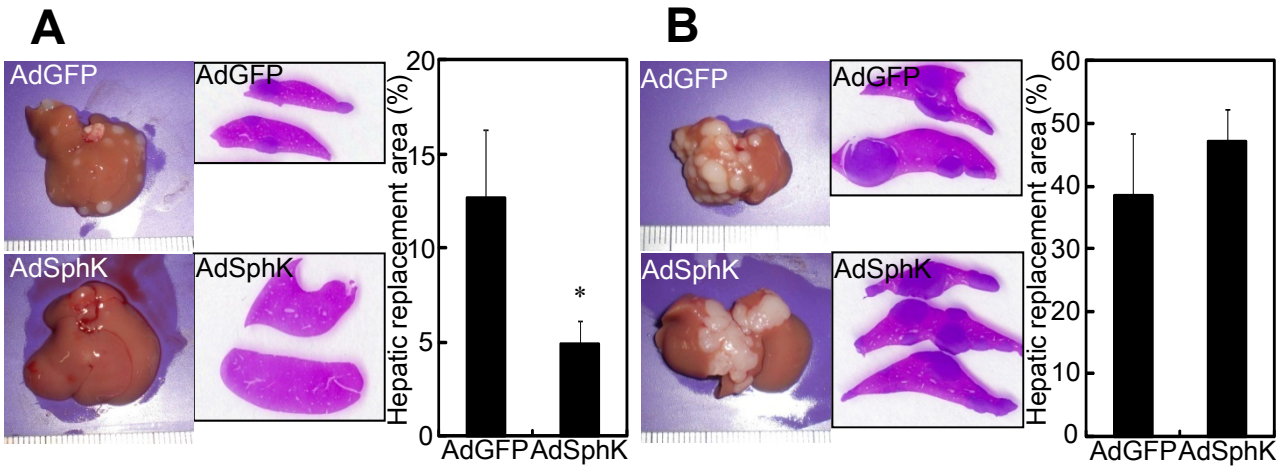

Supplementary Figure 5. SphK overexpression decreased metastatic tumor growth in the liver. (A) Wild-type mice were infected with AdGFP (upper panels) or AdSphK (lower panels) 24 h before cell inoculation, intrasplenically injected with SL4 (2×10^4 cells), and sacrificed 14 d after inoculation. (B) Wild-type mice were intrasplenically injected with SL4 (2×10^4 cells), infected with AdGFP (upper panels) or AdSphK (lower panels) 5 d after inoculation, and sacrificed 14 d after infection (19 d after SL4 inoculation). Photograph of the liver after excision. Liver sections were stained with H&E (loupe magnification) and intrahepatic tumor load was presented as hepatic replacement area based on the measurement of 3 non-sequential sections. Results are given as means ± SD of data collected from at least 5 independent experiments. *$P < 0.05$ using a 2-tailed Student's *t*-test.

Supplementary Figure 6

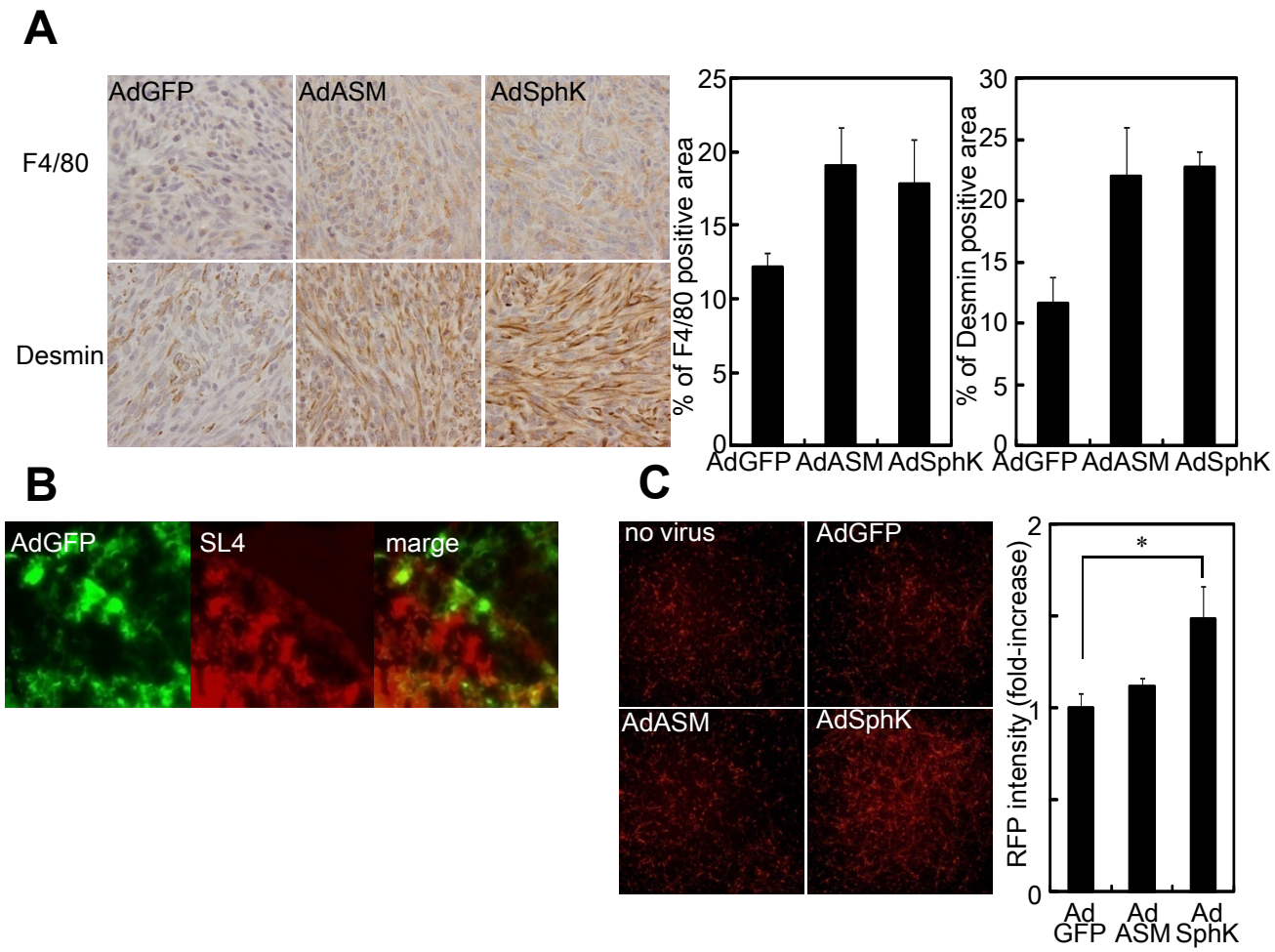

Supplementary Figure 6. SphK stimulated the proliferation of colon cancer cells. (A) Wild-type mice were intrasplenically injected with SL4 (2 × 10^4 cells), infected with AdGFP (left panels), AdASM (middle panel), or AdSphK (right panels) 5 d after inoculation, and sacrificed 14 d after infection (19 d after SL4 inoculation). Expression of F4/80 in the metastatic tumor (upper panels) and desmin (lower panels) around the tumor invasive margin (original magnification: 400×) was examined by immunohistochemistry, and measurement of immunostain-positive area was performed. (B) Wild-type mice were intrasplenically injected with SL4 (2 × 10^4 cells), infected with AdGFP 5 d after inoculation, and sacrificed 3 d after infection (8 d after SL4 inoculation). For detection of RFP fluorescence, unfixed liver was embedded in OCT, before frozen sections were cut on a cryostat and AdGFP-derived GFP and RFP (SL4) expression in the unfixed frozen liver was assessed by fluorescent microscopy. Each panel shows the same field of the border of the metastatic tumor and liver (original magnification: 400×). (C) After SL4 cells had been plated on 6-well plates (2 × 10^5 cells/well), some cells were infected with AdGFP, AdASM, or AdSphK. At 48 h after infection, RFP (SL4) was observed with a fluorescent microscope (left panels). Cells were sonicated in 1% Triton-X containing PBS and the fluorescent intensity of RFP (544/590) was assessed with a fluorometer. Results are presented as means ± SD of data collected from at least 5 independent experiments. *P < 0.05 using a 2-tailed Student's *t*-test.

Supplementary Figure 7

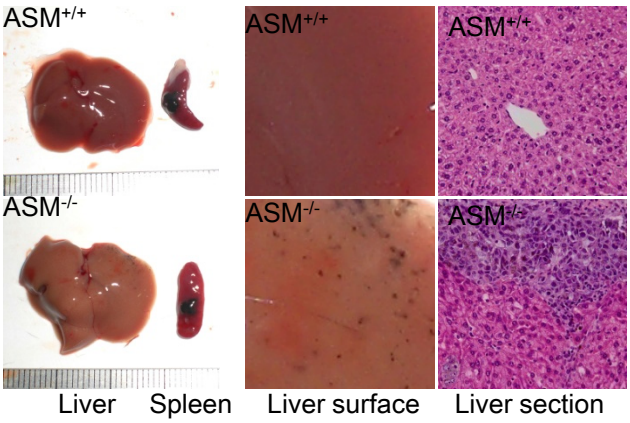

Supplementary Figure 7. B16C2M cells formed metastatic liver tumors in the *ASM*$^{-/-}$ liver. *ASM*$^{+/+}$ (upper panels) and *ASM*$^{-/-}$ (lower panels) mice were intrasplenically injected with B16C2M (1×10^6 cells) and sacrificed 7 d after inoculation. A photograph of the liver and spleen after excision (left panels). A pigmented tumor was observed in the spleens of both *ASM*$^{+/+}$ and *ASM*$^{-/-}$ mice. Loupe magnification of liver surface (middle panels). Liver sections were stained with H&E (right panels, original magnification: 200×).

Supplementary Table 1

Changes in mRNA expression of biomarkers of classically activated and regulatory macrophages.

After wild-type mice had been intrasplenically injected with SL4 (5×10^5 cells) and sacrificed 7 d after inoculation, expression of the indicated mRNA variants in the liver was determined by quantitative real-time RT-PCR. Results are presented as means ± SD of data collected from 5 independent experiments. *P < 0.05 using a 2-tailed Student's *t*-test.

Markers	(-)	SL4
Classically activated		
CD11c	1.00 ± 0.28	7.24 ± 1.93*
IL-12 p40	1.00 ± 0.55	12.44 ± 3.69*
IFN-γ	1.00 ± 1.00	10.17 ± 2.77*
Regulatory		
CD163	1.00 ± 0.28	1.60 ± 0.16*
Mannose receptor	1.00 ± 0.58	2.05 ± 0.25*
IL-10	1.00 ± 0.98	2.54 ± 0.59

Supplementary Table 2

Changes in the mRNA profiles of SL4-inoculated mice

After wild-type mice had been intrasplenically injected with SL4 (5×10^5 cells) and sacrificed 7 d after inoculation, expression of the indicated mRNA variants in the liver was determined by quantitative real-time RT-PCR. Results are presented as means ± SD of data collected from 5 independent experiments. *P < 0.05 versus SL4-inoculated *ASM*$^{+/+}$ mice using a 2-tailed Student's t-test.

			SL4	
	ASM$^{+/+}$	ASM$^{-/-}$	ASM$^{+/+}$	ASM$^{-/-}$
TNF-α	1.00 ± 0.44	2.51 ± 1.27	12.33 ± 3.52	8.07 ± 1.07
IL-1β	1.00 ± 0.69	0.85 ± 0.39	7.76 ± 1.70	2.26 ± 0.83*
CXCL1	1.00 ± 0.25	0.88 ± 0.42	6.98 ± 2.94	3.54 ± 1.47*
CCL5	1.00 ± 0.16	1.65 ± 0.30	3.03 ± 0.57	3.70 ± 1.41
TGF-β	1.00 ± 0.18	1.28 ± 0.29	3.45 ± 0.76	2.34 ± 0.69*
Desmin	1.00 ± 1.07	0.45 ± 0.08	3.85 ± 0.59	1.51 ± 0.29*
α-SMA	1.00 ± 0.80	0.32 ± 0.23	13.90 ± 3.06	7.60 ± 3.13*
Collagen α1(I)	1.00 ± 0.85	0.50 ± 0.28	7.19 ± 1.37	2.90 ± 1.15*
MMP-2	1.00 ± 0.73	0.53 ± 0.20	3.90 ± 1.91	4.83 ± 2.33
MMP-9	1.00 ± 0.84	0.26 ± 0.13	9.70 ± 4.90	14.40 ± 8.75
MMP-13	1.00 ± 0.73	1.42 ± 0.94	14.63 ± 5.40	22.32 ± 6.08

Supplementary Table 3

Lack of effect of S1P on mRNA profiles of macrophages

After isolated $CD11b^+$ macrophages had been plated in DMEM containing 10% FCS and incubated for 1 h, some cells were stimulated with S1P (1 μM) for 4 h and the expression of the indicated mRNA variants was determined by quantitative real-time RT-PCR. LPS was used as a positive control. Results are presented as means ± SD of data collected from 5 independent experiments. *P < 0.05 versus DMSO using a 2-tailed Student's *t*-test.

	DMSO	S1P	LPS
TNF-α	1.00 ± 0.44	0.88 ± 0.20	6.35 ± 0.22*
IL-1β	1.00 ± 0.19	0.90 ± 0.38	13.33 ± 4.73*
CXCL1	1.00 ± 0.32	1.49 ± 0.24	2.37 ± 0.17*
TGF-β	1.00 ± 0.14	1.23 ± 0.11	1.11 ± 0.09
IL-12 p40	1.00 ± 0.37	1.19 ± 0.12	1.00 ± 0.31
IL-10	1.00 ± 0.30	0.61 ± 0.06	4.82 ± 0.80*